JPET Fast Forward. Published on June 16, 2021 as DOI: 10.1124/jpet.121.000530
This article has not been copyedited and formatted. The final version may differ from this version.

Title Page

NOSE-TO-BRAIN DELIVERY OF DEXAMETHASONE: BIODISTRIBUTION STUDIES IN MICE

Iván Nicolás Pérez Osorio [A], Alejandro Espinosa [A], Manuel Giraldo Velázquez [A], Patricia Padilla [A], Brandon Bárcena [A], Gladis Fragoso [A], Helgi Jung-Cook [D], Hugo Besedovsky [B], Gabriela Meneses [C] and Edda Lydia Sciutto Conde [A].

[A]Instituto de Investigaciones Biomédicas, Universidad Nacional Autónoma de México, Mexico City.

[B]Research Group Immunophysiology, Division of Neurophysiology, Institute of Physiology and Pathophysiology. Philipps Universität, (HOB), Marburg, Germany.

[C]Departament of Parasitology. Instituto de Diagnóstico y Referencia Epidemiológicos, Secretaría de Salud, Mexico City.

[D]Facultad de Químicas, Universidad Nacional Autónoma de México, Mexico City.

JPET Fast Forward. Published on June 16, 2021 as DOI: 10.1124/jpet.121.000530
This article has not been copyedited and formatted. The final version may differ from this version.

Running Title Page

BIODISTRIBUTION OF INTRANASALLY ADMINISTERED DEXAMETHASONE IN MICE

Send correspondence to: Edda Sciutto, PhD, Department of Immunology, Instituto de Investigaciones Biomédicas, Universidad Nacional Autónoma de México, Circuito escolar s/n, 04510 Coyoacán, Mexico City, Mexico, 5622-3153; E-mail: edda@unam.mx

Text pages:

Number of tables: 0

Number of figures: 5

Number of references: 33

Number of words in abstract: 194

Number of words in introduction: 317

Number of words in discussion: 1324

Key words: glucocorticoids, intranasal, drug-delivery, neuroinflammation.

Abbreviations

Neuroinflammation (NI), glucocorticoids (GCs), intranasal (IN), intravenous (IV), central nervous system (CNS), dexamethasone (Dex), Tris-buffered saline (TBS), average fluorescence intensity (AFI), phosphate-buffered saline (PBS), blood brain barrier (BBB).

Section assignment: Neuropharmacology

JPET Fast Forward. Published on June 16, 2021 as DOI: 10.1124/jpet.121.000530
This article has not been copyedited and formatted. The final version may differ from this version.

Abstract

Neuroinflammation (NI) is an important physiological process which promotes the tissue repair and homeostatic maintenance in the central nervous system (CNS) after different types of insults. However, when it is exacerbated and sustained in time, NI plays a critical role in the pathogenesis of different neurological diseases. The high systemic doses required for brain-specific targeting leads to severe undesirable effects. The intranasal (IN) route has been proposed as an alternative drug administration route for a better NI control. Herein, the brain biodistribution of intranasally administered dexamethasone (Dex) versus intravenous administered one is reported. A higher amount of dexamethasone was found in every brain analyzed regions of those brains of intranasally administered mice. HPLC analysis also revealed that IN administration allows Dx arrives faster and in a greater concentration to the brain in comparison with intravenous administration, data confirmed by immunofluorescence and HPLC analysis. These data support the proposal of the IN administration of Dx as an alternative for a more efficiently control of NI.

JPET Fast Forward. Published on June 16, 2021 as DOI: 10.1124/jpet.121.000530
This article has not been copyedited and formatted. The final version may differ from this version.

Significant statement

This work highlights the biodistribution of dexamethasone after its intranasal administration. Intranasal administration allows for a faster arrival, better distribution and a higher concentration of the drug within the brain compared to its intravenous administration. These results explain some of the evidence shown by us in a previous work in which dexamethasone controls neuroinflammation in a murine stroke model and can be used to propose alternative treatments for neuroinflammatory diseases.

JPET Fast Forward. Published on June 16, 2021 as DOI: 10.1124/jpet.121.000530
This article has not been copyedited and formatted. The final version may differ from this version.

INTRODUCTION

Neuroinflammation (NI), is an inflammatory process that is present in the central nervous system, and is a common feature of different neurological diseases. In many of these pathologies, it is clearly associated with its pathogenesis. However, NI is almost treated only when it is exacerbation leads the patient's life at risk. A limitation for its treatment is the low efficiency of the available therapies. Synthetic glucocorticoids (GCs) are powerful immunosuppressive drugs for controlling inflammation(Cain and Cidlowski, 2017). In spite of being the most extensively drugs for controlling inflammation, the available marketed GCs are in oral and intravenous (IV) presentations that have a low brain-targeting efficiency. Thus, high doses of GCs are required to reach the therapeutic central levels. GCs are secreted naturally by our adrenal gland in response to stress and have numerous effects in metabolic pathways essential for life. Consequently, the high doses required to reach central nervous system (CNS), results in multiple negative side effects in peripheral tissues(Oray *et al.*, 2016). This panorama points the clear need to improve GC brain-targeting. One novel alternative to address this challenge is the intranasal (IN) delivery. This route can transport GC directly to the central nervous system through the olfactory and trigeminal nerves bypassing the blood-brain barrier (BBB)(Erdő *et al.*, 2018a). In addition, the IN route avoids the first-pass metabolism and gastrointestinal degradation when oral administered(Gibaldi *et al.*, 1971)·(Erdő *et al.*, 2018b) or the cost and inconvenience and possible complications that arise when intravenously administered. Intranasal delivery has been reported as a safe alternative to the parenteral administration of different drugs(Erdő *et al.*, 2018b). Indeed, we first demonstrated the higher efficiency of the IN than the intravenous route to control NI in an experimental murine model of aseptic sepsis(Meneses, Gevorkian, Florentino, M. A.

JPET Fast Forward. Published on June 16, 2021 as DOI: 10.1124/jpet.121.000530
This article has not been copyedited and formatted. The final version may differ from this version.

Bautista, *et al.*, 2017; Meneses *et al.*, 2019) and in the experimental autoimmune encephalitis(Rassy *et al.*, 2020).

Considering these data, in this study we extended the knowledge of the IN administration of GC through the study of the drug brain distribution in mice following intranasal administration of dexamethasone, one of the most extensively used GC to control NI.

JPET Fast Forward. Published on June 16, 2021 as DOI: 10.1124/jpet.121.000530
This article has not been copyedited and formatted. The final version may differ from this version.

MATERIALS AND METHODS

Mice

Male C57BL/6 mice, aged 7–8 weeks (approximately 36 g body weight), purchased from Harlan-México (Ciudad de México, México) and further bred at Instituto de Investigaciones Biomédicas (IIB), were employed. For in vivo experiments, male CD1 nu/nu mice (purchase at Instituto Nacional de Ciencias Médicas y Nutrición Salvador Zubirán bioterium) of 6-8 weeks old were employed. All mice were kept in plexiglass boxes with food (Teklad Sani-Chips® 7090) and water (filtered, acidified and sterilized) ad libitum in groups of five to six animals before and during the experiments. The animal room was maintained at 22 ± 3°C with a 12/12 hours light–dark cycle. The number of mice used in each individual experiment are mentioned in the respective figure.

All housing and experimental procedures were conducted under the guidelines established by the Committee on the Care and Use of Experimental Animals of the IIB at the Universidad Nacional Autónoma de México (UNAM) and by the U.S. National Institutes of Health. Experimentation protocol was approved by the animal safety and ethical committee of the IIB, UNAM (Protocol Number approval ID 140).

Glucocorticoids Treatment

For IN and IV administration groups of 5 mice were anesthetized with an intraperitoneal injection of Ketamine-Xylazine (3:1). A dose of 0.25 mg/Kg (2.25:17.75 µL Dex:saline solution) of Dexamethasone (Dex) Alin® (Disodium phosphate of Dexamethasone 8mg/2ml) was inoculated by drip with a micropipette into each nostril of the mice for IN administration.

JPET Fast Forward. Published on June 16, 2021 as DOI: 10.1124/jpet.121.000530
This article has not been copyedited and formatted. The final version may differ from this version.

For the IV administration, Dex was injected at the same dose (2.25:47.75 µL Dex:saline solution) through the tail vein. 24 hours after Dx administration, the mice were sacrificed for brains collection and their further analysis by immunofluorescence and tissue transparency. Serum was obtained by differential centrifugation from blood samples at 15,000 rpm. The brains were quickly rinsed with isotonic saline solution and fixed in paraformaldehyde or used to prepare homogenates for further analysis. Samples were stored at -20 °C until HPLC analysis. The same anesthesia procedure mentioned above and the mice handing was performed for intranasally and intravenously inoculated animals and for brain transparency experiments.

Immunofluorescence

We divided each mouse brain in 8 sections taking Bregma as an anatomical reference (Fig. 1A), to have representative sections of all brain structures, areas at 3.92, 2.80, 1.98, 1.34, 0.62, -0.22, -1.70 and -2.80 mm from Bregma were selected and analyzed. For immunofluorescence stains, brains from either IN or IV Dex treated mice were fixed in 4% buffered paraformaldehyde at 4°C overnight. Free-floating 30 µm-thick mouse to brain sections were processed as described previously(Meneses, Gevorkian, Florentino, M. A. Bautista, *et al.*, 2017). After antigen retrieval by incubating in sodium citrate buffer (10 mM Sodium citrate, 0.05% Tween 20, pH 6.0) at 70°C for 50 min, samples were washed thoroughly several times with Tris-buffered saline (TBS) and blocked with a solution of 2% immunoglobulin (Ig)G-free albumin (Sigma, St Louis, MO, USA) in TBS for 20 min at room temperature. Sections were then incubated overnight at 4°C with rabbit anti-dexamethasone antibody (1:250, Abcam, Cambridge, UK) to study Dex distribution. This antibody has been chosen as it has been reported to have high specificity against dexamethasone(Graversen *et al.*, 2012; Grewal *et al.*, 2013; Yang *et al.*, 2018). Mouse anti-GFAP (1:1000) antibody (#130300, Thermo Fisher Scientific, USA) was used to analyze if astrocytes internalize Dex.

JPET Fast Forward. Published on June 16, 2021 as DOI: 10.1124/jpet.121.000530
This article has not been copyedited and formatted. The final version may differ from this version.

After washing, the former sections were incubated for 1 h at room temperature with Alexa Fluor 594 goat anti-rabbit IgG (1:250, Molecular Probes, Eugene, OR, USA). Another group additionally was incubated with 1:250 Alexa Fluor 488 rat anti-mouse IgG (#A21131, Thermo Fisher Scientific USA), both diluted in TBS–2% BSA. Samples were mounted onto glass slides in Vectashield medium (Vector Laboratories, Burlingame, CA, USA) containing 4',6-diamidino-2-phenylindole (DAPI) for nuclei imaging. Images were processed using Image J software (National Institute of Health, Bethesda, MD, USA), with which the coverage as well as the average fluorescence intensity (AFI) of the administered Dex were analyzed. For the Dex biodistribution analysis, immunofluorescence stains were analyzed using an Olympus BX51-WI microscope and for the intracellular distribution of Dex a Confocal Nikon A1R+ STORM microscope was used.

Brain transparency

To visualize the distribution of Dex with a three-dimensional perspective, a brain transparency protocol was performed as previously reported(Xu *et al.*, 2017). Mice were transcardially perfused with 40mL ice-cold phosphate-buffered saline (PBS) solution (1M, pH 7.6) followed by 20mL of 4% (wt/vol) PFA in 1M PBS. After collecting 1 mm coronal sections with a mouse brain mold, the brain slices were post-fixed in the same fixative solution at 4°C for 3 days. The slices were cleared 4% (wt/vol) SDS in sodium borate buffer (200mM; pH 8.5) at 37 °C with gentle rotational shaking. The solutions were refreshed daily until visual confirmation of complete tissue transparency by viewing black grid lines on a white sheet of paper through the tissue itself.

High performance liquid chromatography

The extraction of Dex from the samples was carried out as previously reported with some modifications(Yuan *et al.*, 2015). Samples were tacked at 15, 60, 180 and 300 minutes after

JPET Fast Forward. Published on June 16, 2021 as DOI: 10.1124/jpet.121.000530
This article has not been copyedited and formatted. The final version may differ from this version.

Dex IN or IV administration. To each brain, a volume of 500 µl of HPLC grade ethanol (Merck, 64-17-5) was added and for serum samples, ethanol was added in 1:1 ratio. The tissues were homogenized at 40 MHz with an ultrasound sonicator (hielscher UP400St) at 4 °C. The homogenates were centrifuged at 12,000 rpm at 4° C for 15 minutes. The supernatant from each sample was recovered and a second extraction was carried out at the same conditions described above. Then, recovered supernatants were lyophilized and reconstituted adding 100 µL of ethanol, 50 µL of acetonitrile and 50 µL of water/acetonitrile (80:20) for its subsequent analysis. Samples were analyzed using a reverse phase HPLC with UV detection and a C18 column Spherisorb ODS2 4.6 X 150 mm (Cat. PSS832113 WATERS), at flow rate 1.0 mL/min, detection wavelength 243 nm and using a mobile phase composed of water-methanol (20:80 ml). The method was linear in the range of 0.781 µg/mL to 12.50 µg/ml. The detected Dex concentration was reported in µg/ml.

Statistical analysis

The statistical analysis of the immunofluorescence data AFI, the coverage of the Dex in the brain and the concentration of Dex in the brain quantified by HPLC was carried out by ANOVA test with a post-hoc analysis of Tukey. All differences were considered significant at $P<0.05$. Data are presented as mean ± standard deviation and statistical analyses were performed with GraphPad InStat (GraphPad Software, San Diego, CA, USA).

Graphical representations were performed using the GraphPad Prism 7 software (GraphPad Software, Inc., USA).

JPET Fast Forward. Published on June 16, 2021 as DOI: 10.1124/jpet.121.000530
This article has not been copyedited and formatted. The final version may differ from this version.

RESULTS

Brain distribution of Dexamethasone

Twenty-four hours after Dex administration, its distribution in the brain was determined by immunofluorescence (Fig. 1C). The slices of mice brains were made taking Bregma as an anatomical reference region as shown in Figure 1A. Analysis were performed in 8 brain sections. As observed, the Dex brain coverage after IN administration was higher than IV one in every analyzed section (Fig 1B). The highest differences between IV vs IN administered Dex coverage was at 0.62, -0.22, -1.70 and -2.80 mm from Bregma (Fig. 1B). A more detailed breakdown sections at 1.34, 0.62 and -0.22 mm from Bregma was performed since they have an especially relevant roll in the motor control of mice and human body, this because these areas include basal ganglia structures like striatum, caudate nucleus, motor cortex, putamen, subthalamic nucleus, and substantia nigra(Groenewegen, 2003). As shown, Dex mainly distributes in the cortex and the caudate nucleus of these areas. As shown in Figure 2, statistically significant differences between IN and IV administration were observed in all analyzed sections (1.34, 0.62 and -0.22 mm from Bregma), except for the cortex at -0.22 mm from Bregma. For striatum brain transparency see supplementary Figure 1. Thus, higher levels of Dex were found in IN vs IV administered.

JPET Fast Forward. Published on June 16, 2021 as DOI: 10.1124/jpet.121.000530
This article has not been copyedited and formatted. The final version may differ from this version.

A simple and highly sensitive HPLC method was developed to determine Dex concentration in brain and blood serum samples (Dex detection limit for this method was 0.11 µg/ml and quantification limit was 0.35 µg/ml), the minimum amount of drug detected in brain was 1.050 µg/ml and in serum 1.108 µg/ml. Figure 3A shows the chromatogram resulting from this assay. Figure 3B shows that 30 minutes after Dex administration, a significantly higher concentration of the drug was detected in the brain of the mice administered intranasally compared to those IV treated. Levels remained statistically higher until 60 minutes. Differences were not observed after 180 minutes post-administration. The opposite was observed in serum, where the highest levels were reached in serum of intravenously Dex administered mice. Regardless the route employed no differences between both treatments were observed at 180 minutes after administration.

Figure 4A depicts the reconstruction of a mouse olfactory bulb after 15 minutes of intranasal administrated Dex. As observed, Dex is widely distributed in the olfactory bulb and also within different cells (Figure 4B). These results indicate the relevance of studying the different cell types in which Dex had been internalized. As shown in Figure 4C and 4D, astrocytes internalize Dex and it is not only distributed inside or around the nucleus but all along the astrocyte soma.

DISCUSSION

Herein, we used Dex (dexamethasone sodium phosphate, a salt form of dexamethasone), a lipophilic synthetic anti-inflammatory and antialgic glucocorticoid metabolized by the cytochrome P450 (CYP) 3A4 within the liver and which elimination occurs via renal excretion. In addition to binding to specific nuclear steroid receptors, dexamethasone also activates NF-kB and apoptotic pathways(Ciobotaru *et al.*, 2019).

JPET Fast Forward. Published on June 16, 2021 as DOI: 10.1124/jpet.121.000530
This article has not been copyedited and formatted. The final version may differ from this version.

A comparison of dexamethasone brain distribution is presented when administered IN vs IV using different experimental approaches. Several studies have reported the bioavailability of different drugs in the central nervous system after intranasal administration. Although, GCs have been widely used due to its powerful and effective anti-inflammatory property, to our knowledge this is the first study that addresses their bioavailability in the CNS when they are intranasally delivered.

The experiments reported in Figures 1, 2 and 4 showed clear higher fluorescence in intranasally administered mice after 24 hours of drug administration. We chose this timepoint because in previous studies, we identified that after 24 hours of its intranasal administration, Dex controls more efficiently neuroinflammation than at shorter periods of time in a sepsis model(Meneses *et al.*, 2017). Meanwhile, HPLC experiments (Figures 3) were analyzed at shorter times, because we couldn`t detect the drug with each technique after 24 of administration. This could be due to the caption of Dex by the glucocorticoid receptor, where is no longer bioavailable. Nevertheless, at shorter times the differences between IN and IV administration remain.

One important finding of this study is that Dex can be rapidly detected and in a higher concentration in the brain when it is intranasally administered in comparison with the intravenous administration. This difference may be related to the fact that intranasally administered Dex can reach the CNS through the olfactory and trigeminal nerves, as shown in Figure 4A. Moreover, drugs like prednisone and Dex are natural substrates for the (mdr) P-glycoprotein (ABC transporter) coded by the MDR1 gene. This transporter favors the efflux of Dex through the BBB regardless of the administration route, however, as the IN route is more efficient to deliver Dex to the CNS than IV route, higher concentrations of the drug remained in intranasally administered mice brains(Meijer *et al.*, 1998; Karssen *et al.*, 2002; Löscher and Potschka, 2005). How P-glycoprotein and Dex interacts after its IN or IV

JPET Fast Forward. Published on June 16, 2021 as DOI: 10.1124/jpet.121.000530
This article has not been copyedited and formatted. The final version may differ from this version.

administration should be analyzed in future studies. Furthermore, when GCs are administered intravenously, a "protein crown" around the drug is formed; when this happens, different proteins such as albumin, α-1 glycoprotein, lipoproteins and α, β and ɣ globulins bind in a reversable way to GCs, which decreases its range of arrival to the brain or to any target organ. In particular, in the case of Dex, it binds initially and mostly to albumin and then to lipoproteins(Peets *et al.*, 1969; Cummings *et al.*, 1990).

Inside mice brain, the drug is mainly distributed in the regions at 1.34, 0.62 and -0.22 mm from Bregma, and as mention above, these areas have neuroanatomical regions which are relevant for the motor control in the brain, and within these areas, the drug is mostly detected in the cortex and caudate nucleus (Fig. 2), except for the cortex at -0.22 mm from Bregma, probably due to a more homogeneous distribution of Dex in the cortex of this area no matter the administration route. A more detailed analysis of the anatomical implications of the Dex biodistribution at -0.22 mm from Bregma should be done. Previous studies demonstrate that molecules administered by the IN route can take its way through the vasculature adjacent to the nasal cavity as well as the trigeminal and olfactory nerves to arrive to the SNC(Lochhead and Thorne, 2012; Crowe *et al.*, 2018). Together, these results and previously reported ones(Espinosa *et al.*, 2020), suggest that IN administration of Dex could be used to recover motor impairment associated to neurological disorders.

Considering the higher amount of Dex in the mentioned regions, the possibility of using this administration route for the treatment of NI in pathologies like the cerebrovascular event is highlighted, especially considering that these regions have been shown to be affected by this pathology, in particular structures from the basal ganglia like the striated nucleus(Longa *et al.*, 1989).

Dex pharmacokinetics was analyzed by HPLC in order to determine if differences between its concentration after IN and IV administration. It was observed that 15 minutes post-

JPET Fast Forward. Published on June 16, 2021 as DOI: 10.1124/jpet.121.000530
This article has not been copyedited and formatted. The final version may differ from this version.

administration, the Dex concentration administered in the brain was higher after the IN administration than after IV administration but in serum the opposite was observed, probably due to a low interaction of the drug with the BBB when it was administered intranasally. Meanwhile, Dex intravenously administered takes longer to reach brain, mainly because it has to pass through BBB, so it takes longer time to get similar Dex levels in the CNS compared with it is administered by the IN route. It has been observed that drugs like Dex reaches their equilibrium faster when a highly vascularized organ is their target, but this phenomenon take place in a lower range when the drug has to cross different cellular membranes to reach its target organ. Additionally, this phenomenon can explain our results at later times. Indeed, after 60 minutes of IV Dex administration, its concentration in serum decreased to values similar to those observed when administered intranasally, at this moment, Dex reached its equilibrium within the CNS(Cummings *et al.*, 1990; Al Katheeri *et al.*, 2006)·(Samtani and Jusko, 2005). As expected, no differences in the levels of Dex were observed between IN and IV administration after 120 minutes post-administration. Overall, these results suggest that Dex availability in to the brain will be faster after its IN administration, time at which it is expected exerts its central anti-inflammatory functions. It is important to note that Dex metabolites were measured in this study at any time, so in future studies the measurement of these metabolites should be carried out to complete the data of intranasally administered Dex. The Dex concentration values shown in this work coincide with those previously reported, where the maximum Dex concentration was detected in plasma 30 minutes after intraperitoneal administration, that became undetectable 10 hours post-administration(Chang-Lin *et al.*, 2011; Cubana *et al.*, 2011; Yuan *et al.*, 2015). High values of Dex detected in mice brains within the first 60 minutes after its IN administration compared to IV administered drug, highlight the possibility of a therapeutic use of Dex in which better drug dosage could be carried out and the control of inflammation in short laps and of time is crucial for the patient recover, like in stroke patients.

JPET Fast Forward. Published on June 16, 2021 as DOI: 10.1124/jpet.121.000530
This article has not been copyedited and formatted. The final version may differ from this version.

Figure 4A and 4B shows an olfactory bulb reconstruction where the distribution of the drug is observed within the microvasculature and an intracellular distribution, demonstrating that after IN administration, Dex pass through the olfactory bulb to reach the brain. To find out how Dex interacts with astrocytes an immunodetection assay was performed. As seen in Figure 4C and 4D, there is an internalization of Dex in astrocytes from basal ganglia which may account to the modulation in the expression of molecules such as pro and anti-inflammatory cytokines, as well as in the response to the stimulation by neurotransmitters(Ciaranello and Axelrod, 1975; Chao *et al.*, 1992; Brenner *et al.*, 1993; Riva *et al.*, 1995, 1998; Rock *et al.*, 2005; Slotkin *et al.*, 2006). A confocal reconstruction of Dex into the astrocytes is presented in supplementary Figure 2 and supplementary Figure 3. Further studies will be conducted to evaluate the effect of Dex on astrocytes and other cell types in different brain regions, so that possible therapeutic foci can be identified.

Another point that merits some comments is that in the present study Dex was solubilized only in saline solution, so it is possible to improve the deposition of the drug in the nasal area and the efficiency to target the olfactory mucosa by its reformulation. Moreover, many advances have been done in the design of a special disposer to be used for IN to Brain delivery that is currently accessible in the market(Djupesland, 2013; Jassim and Al-akkam, 2018).

JPET Fast Forward. Published on June 16, 2021 as DOI: 10.1124/jpet.121.000530
This article has not been copyedited and formatted. The final version may differ from this version.

CONCLUSIONS

In this study the *in vivo* biodistribution of intranasally administered Dex is reported, a knowledge that will contribute to expand its use for the control of NI event associated with different pathologies using very low doses of steroids and therefore reducing its possible negative peripheral side effects. More detailed research should be performed to elucidate the specific mechanisms that are carried out by Dex to control NI in different pathological conditions.

CONFLICT OF INTEREST

No author has an actual or perceived conflict of interest with the contents of this article.

JPET Fast Forward. Published on June 16, 2021 as DOI: 10.1124/jpet.121.000530
This article has not been copyedited and formatted. The final version may differ from this version.

ACKNOWLEDGMENTS

The authors thank Pedro Medina, Marisela Hernández, Miguel Tapia and Laura Montero for their technical support, and Daniel Garzón for the assistance with animal care. Iván Nicolás Pérez-Osorio obtained his master from Programa de Maestría en Ciencias Biológicas, Universidad Nacional Autónoma de México, and received a fellowship from CONACYT. This work was supported by DGAPA-UNAM (IN207720 to E.S.) Mexico. This study was also supported by the institutional program “Programa de Investigación para el Desarrollo y la Optimización de Vacunas, Inmunomoduladores y Métodos Diagnósticos del IIB” (PROVACADI).

JPET Fast Forward. Published on June 16, 2021 as DOI: 10.1124/jpet.121.000530
This article has not been copyedited and formatted. The final version may differ from this version.

Authorship contribution

Participated in research design: Pérez-Osorio I.N., Sciutto E., Fragoso G.

Conducted experiments: Pérez-Osorio I.N., Giraldo Velázquez M., Bárcena B., Espinoza A.

Contributed new reagents or analytic tools: Padilla P., Besedovsky H.

Performed data analysis: Pérez-Osorio I.N., Meneses G., Jung-Cook H.

Wrote or contributed to the writing of the manuscript: Pérez-Osorio I.N., Sciutto E., Fragoso G.

JPET Fast Forward. Published on June 16, 2021 as DOI: 10.1124/jpet.121.000530
This article has not been copyedited and formatted. The final version may differ from this version.

REFERENCES

Al Katheeri NA, Wasfi IA, Lambert M, Giuliano Albo A, and Nebbia C (2006) In vivo and in vitro metabolism of dexamethasone in the camel. *Vet J* **172**:532–543.

Brenner T, Yamin A, Abramsky O, and Gallily R (1993) Stimulation of tumor necrosis factor-α production by mycoplasmas and inhibition by dexamethasone in cultured astrocytes. *Brain Res* **608**:273–279, Elsevier.

Cain DW, and Cidlowski JA (2017) Immune regulation by glucocorticoids. *Nat Rev Immunol* **17**:233–247.

Chang-Lin JE, Attar M, Acheampong AA, Robinson MR, Whitcup SM, Kuppermann BD, and Welty D (2011) Pharmacokinetics and pharmacodynamics of a sustained-release dexamethasone intravitreal implant. *Investig Ophthalmol Vis Sci* **52**:80–86, The Association for Research in Vision and Ophthalmology.

Chao CC, Hu S, Close K, Choi CS, Molitor TW, Novick WJ, and Peterson PK (1992) Cytokine Release from Microglia: Differential Inhibition by Pentoxifylline and Dexamethasone. *J Infect Dis* **166**:847–853, Narnia.

Ciaranello RD, and Axelrod J (1975) EFFECTS OF DEXAMETHASONE ON NEUROTRANSMITTER ENZYMES IN CHROMAFFIN TISSUE OF THE NEWBORN RAT. *J Neurochem* **24**:775–778, John Wiley & Sons, Ltd (10.1111).

Ciobotaru OR, Lupu MN, Rebegea L, Ciobotaru OC, Duca OM, Tatu AL, Voinescu CD, Stoleriu G, Earar K, and Miulescu M (2019) Dexamethasone - Chemical structure and mechanisms of action in prophylaxis of postoperative side effects. *Rev Chim* **70**:843–847.

Crowe TP, Greenlee MHW, Kanthasamy AG, and Hsu WH (2018) Mechanism of intranasal drug delivery directly to the brain, Pergamon.

Cubana R, Sanitario R, Farmac GE, Finlay CJ, and Hipersensibilidad C (2011) Dexametasona 8 mg. *Rev Cuba Farm* **45**:313–317, [Centro Nacional de Información de Ciencias Médicas.].

Cummings DM, Larijani GE, Conner DP, Ferguson RK, and Rocci ML (1990) Characterization of dexamethasone binding in normal and uremic human serum. *DICP, Ann Pharmacother* **24**:229–231.

Djupesland PG (2013) Nasal drug delivery devices: Characteristics and performance in a clinical perspective-a review. *Drug Deliv Transl Res* **3**:42–62.

Erdő F, Bors LA, Farkas D, Bajza Á, and Gizurarson S (2018a) Evaluation of intranasal delivery route of drug administration for brain targeting. *Brain Res Bull* **143**:155–170.

Erdő F, Bors LA, Farkas D, Bajza Á, and Gizurarson S (2018b) Evaluation of intranasal delivery route of drug administration for brain targeting, Elsevier.

Espinosa A, Meneses G, Chavarría A, Mancilla R, Pedraza-Chaverri J, Fleury A, Bárcena B, Pérez-Osorio IN, Besedovsky H, Arauz A, Fragoso G, and Sciutto E (2020) Intranasal Dexamethasone Reduces Mortality and Brain Damage in a Mouse Experimental Ischemic Stroke Model. *Neurotherapeutics* **17**:1907–1918.

Gibaldi M, Boyes RN, and Feldman S (1971) Influence of First-Pass Effect on Availability

of Drugs on Oral Administration. *J Pharm Sci* **60**:1338–1340, John Wiley & Sons, Ltd.

Graversen JH, Svendsen P, Dagnæs-Hansen F, Dal J, Anton G, Etzerodt A, Petersen MD, Christensen PA, Møller HJ, and Moestrup SK (2012) Targeting the hemoglobin scavenger receptor CD163 in macrophages highly increases the anti-inflammatory potency of dexamethasone. *Mol Ther* **20**:1550–1558, Nature Publishing Group.

Grewal AS, Nedzelski JM, Chen JM, and Lin VYW (2013) Dexamethasone uptake in the murine organ of Corti with transtympanic versus systemic administration. *J Otolaryngol - Head Neck Surg* **42**:1.

Groenewegen HJ (2003) The basal ganglia and motor control. *Neural Plast* **10**:107–120.

Jassim ZE, and Al-akkam EJ (2018) Review Article A review on strategies for improving nasal drug delivery systems. *Drug Invent Today* **10**:1–9.

Karssen AM, Meijer OC, Van Der Sandt ICJ, De Boer AG, Lange D, and De Kloet ER (2002) *The role of the efflux transporter P-glycoprotein in brain penetration of prednisolone*.

Lochhead JJ, and Thorne RG (2012) Intranasal delivery of biologics to the central nervous system, Elsevier.

Longa EZ, Weinstein PR, Carlson S, and Cummins R (1989) Reversible middle cerebral artery occlusion without craniectomy in rats. *Stroke* **20**:84–91.

Löscher W, and Potschka H (2005) Blood-brain barrier active efflux transporters: ATP-binding cassette gene family. *NeuroRx* **2**:86–98, American Society for Experimental Neurotherapeutics.

Meijer OC, De Lange ECM, Breimer DD, De Boer AG, Workel JO, and De Kloet ER (1998) Penetration of dexamethasone into brain glucocorticoid targets is enhanced in mdr1A

P-glycoprotein knockout mice. *Endocrinology* **139**:1789–1793.

Meneses G, Cárdenas G, Espinosa A, Rassy D, Pérez-Osorio IN, Bárcena B, Fleury A, Besedovsky H, Fragoso G, and Sciutto E (2019) Sepsis: Developing new alternatives to reduce neuroinflammation and attenuate brain injury.

Meneses G, Gevorkian G, Florentino A, Bautista M. A., Espinosa A, Acero G, Díaz G, Fleury A, Pérez Osorio IN, del Rey A, Fragoso G, Sciutto E, and Besedovsky H (2017) Intranasal delivery of dexamethasone efficiently controls LPS-induced murine neuroinflammation. *Clin Exp Immunol* **190**:304–314, John Wiley & Sons, Ltd (10.1111).

Meneses G, Gevorkian G, Florentino A, Bautista M.A., Espinosa A, Acero G, Díaz G, Fleury A, Pérez Osorio IN, del Rey A, Fragoso G, Sciutto E, and Besedovsky H (2017) Intranasal delivery of dexamethasone efficiently controls LPS-induced murine neuroinflammation. *Clin Exp Immunol* **190**.

Oray M, Abu Samra K, Ebrahimiadib N, Meese H, and Foster CS (2016) Long-term side effects of glucocorticoids. *Expert Opin Drug Saf* **15**:457–465.

Peets A, Staub M, and Symchowics S (1969) Plasma binding of Betamethasone-3H, Dexamethasone-3H and Cortisol-14C. A comparative study. Biochemical Pharmacology. *Biochem Pharmacol* **18**:1655–1663.

Rassy D, Bárcena B, Pérez-Osorio IN, Espinosa A, Peón AN, Terrazas LI, Meneses G, Besedovsky HO, Fragoso G, and Sciutto E (2020) Intranasal Methylprednisolone Effectively Reduces Neuroinflammation in Mice With Experimental Autoimmune Encephalitis. *J Neuropathol Exp Neurol* **79**:226–237.

Riva MA, Fumagalli F, and Racagni G (1995) Opposite Regulation of Basic Fibroblast

Growth Factor and Nerve Growth Factor Gene Expression in Rat Cortical Astrocytes Following Dexamethasone Treatment. *J Neurochem* **64**:2526–2533, John Wiley & Sons, Ltd (10.1111).

Riva MA, Molteni R, and Racagni G (1998) Differential regulation of FGF-2 and FGFR-1 in rat cortical astrocytes by dexamethasone and isoproterenol. *Mol Brain Res* **57**:38–45, Elsevier.

Rock RB, Hu S, Gekker G, Sheng WS, May B, Kapur V, and Peterson PK (2005) Mycobacterium tuberculosis– Induced Cytokine and Chemokine Expression by Human Microglia and Astrocytes: Effects of Dexamethasone. *J Infect Dis* **192**:2054–2058, Narnia.

Samtani MN, and Jusko WJ (2005) Comparison of dexamethasone pharmacokinetics in female rats after intravenous and intramuscular administration. *Biopharm Drug Dispos* **26**:85–91, John Wiley & Sons, Ltd.

Slotkin TA, Kreider ML, Tate CA, and Seidler FJ (2006) Critical prenatal and postnatal periods for persistent effects of dexamethasone on serotonergic and dopaminergic systems. *Neuropsychopharmacology* **31**:904–911, Nature Publishing Group.

Xiong B, Li A, Lou Y, Chen S, Long B, Peng J, Yang Z, Xu T, Yang X, Li X, Jiang T, Luo Q, and Gong H (2017) Precise cerebral vascular atlas in stereotaxic coordinates of whole mouse brain. *Front Neuroanat* **11**:1–17.

Xu N, Tamadon A, Liu Y, Ma T, Leak RK, Chen J, Gao Y, and Feng Y (2017) Fast free-of-acrylamide clearing tissue (FACT) - An optimized new protocol for rapid, high-resolution imaging of three-dimensional brain tissue. *Sci Rep* **7**:1–15.

Yang KJ, Son J, Jung SY, Yi G, Yoo J, Kim DK, and Koo H (2018) Optimized

phospholipid-based nanoparticles for inner ear drug delivery and therapy. *Biomaterials* **171**:133–143, Elsevier Ltd.

Yuan Y, Zhou X, Li J, Ye S, Ji X, Li L, Zhou T, and Lu W (2015) Development and validation of a highly sensitive LC-MS/MS method for the determination of dexamethasone in nude mice plasma and its application to a pharmacokinetic study. *Biomed Chromatogr* **29**:578–583, John Wiley & Sons, Ltd.

Footnotes

This work was supported by Dirección General de Personal Académico, UNAM (DGAPA-UNAM, grant IN 211917 and PAPIIT IV201020), Mexico. This study was also supported by the Institutional program "Programa de Investigación para el Desarrollo y la Optimización de Vacunas, Inmunomoduladores y Métodos Diagnósticos del Instituto de Investigaciones Biomédicas" U.N.A.M.

JPET Fast Forward. Published on June 16, 2021 as DOI: 10.1124/jpet.121.000530
This article has not been copyedited and formatted. The final version may differ from this version.

Legends for Figures

Figure 1. Dex distribution in the mouse brain. A) Lateral view of a mouse brain indicating the distance from Bregma of the cuts that correspond to the sections analyzed by immunofluorescence. Brain image from a Vascular Stereotaxic Atlas(Xiong *et al.*, 2017) B) Intranasally administered Dex showed higher coverage area and statistically significant differences in all analyzed regions compared to intravenous administration. Regions at 0.62, -0.22, -1.70 and -2.80 mm from Bregma presented the higher statistically significant differences ("****" $P<0.01$). C) Red immunofluorescence stained by Alexa Fluor 594 that indicates the presence of Dex in all the analyzed brain regions when IN administered in comparison to the IV administration. These areas include corpus callosum, striatum, motor cortex, putamen and lateral and third ventricles. Each analyzed section has a n=3 for both, IN and IV administration. Scale bar length is 500 μm.

Figure 2. A) Immunostained coronal slice of the cortex and caudate nucleus of mouse brain. A higher level of fluorescence was observed in the cortex and in the caudate nucleus in those mice that received IN Dex. Scale bar length is 500 μm. B) Dex immunofluorescence was estimated in brain sections analyzed at 1.34, 0.62 and -0.22 mm from Bregma. A statistically significant higher AFI was detected in caudate nucleus and cortex at 1.34 mm ("*" $P=0.029$, "**" $P=0.0028$) and 0.62 mm ("***" $P=0.0002$, "****" $P=0.0001$) from Bregma, while at -0.22 mm ("**" $P=0.007$) from Bregma significant differences were observed only in caudate nucleus. Each analyzed section has a n=3 for both, IN and IV administration.

JPET Fast Forward. Published on June 16, 2021 as DOI: 10.1124/jpet.121.000530
This article has not been copyedited and formatted. The final version may differ from this version.

Figure 3. Dex concentration in sera and brain of mice previously administered by IN or IV route with Dex. A) A Representative chromatogram of Dex detected is depicted. B) Levels of Dex in sera and brains of mice at different time after IN or IV Dex administration. During the first 60 minutes after its administration, intranasal administered Dex shows a grater bioavailability within the brain than intravenously administered one ("*" P=0.0132, "**" P=0.0089, "****" P=0.0001). Each analyzed time has a n=5 for both, IN and IV administration.

Figure 4. Dex biodistribution in mouse olfactory bulb and internalization in astrocytes and other cell types. A) Immunofluorescence showing the distribution of Dex in the mouse olfactory bulb. In red Dex and in blue cell nuclei. Scale bar length is 500 μm. B) Cell magnification showing internalization of Dex in cell cytoplasm and nucleus of different cells. Scale bar length is 10 μm. C) Internalization of Dex in astrocytes. Merged signal between Dex (red) and GFAP+ cells (green), nuclei shown in blue. Scale bar length is 20 μm. D) Confocal image showing with a higher detail the intracellular distribution of Dex in astrocytes. View a video for this reconstruction in supplementary figure 2 and 3.

JPET Fast Forward. Published on June 16, 2021 as DOI: 10.1124/jpet.121.000530
This article has not been copyedited and formatted. The final version may differ from this version.

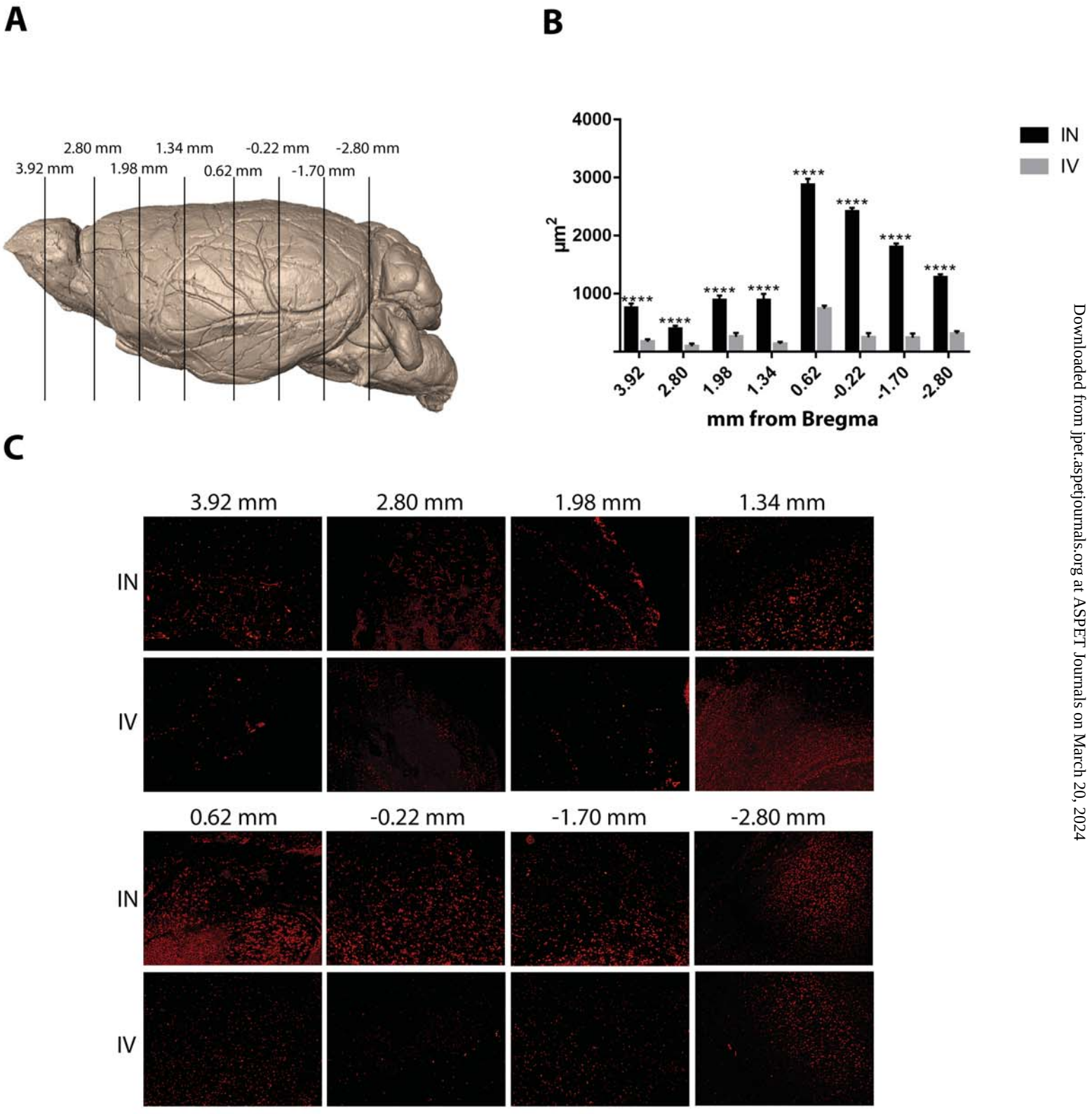

JPET Fast Forward. Published on June 16, 2021 as DOI: 10.1124/jpet.121.000530
This article has not been copyedited and formatted. The final version may differ from this version.

Figure 2

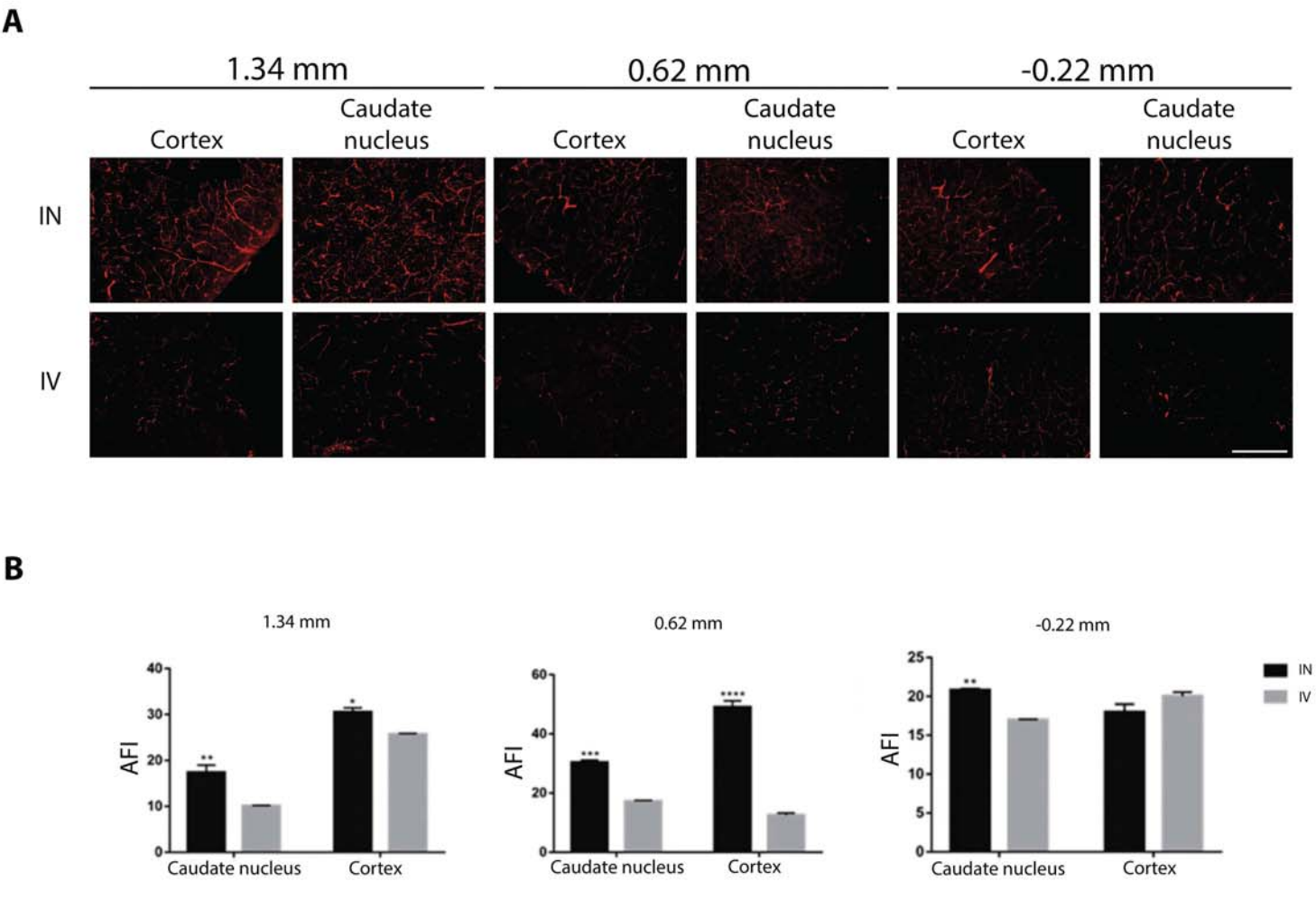

JPET Fast Forward. Published on June 16, 2021 as DOI: 10.1124/jpet.121.000530
This article has not been copyedited and formatted. The final version may differ from this version.

Figure 3

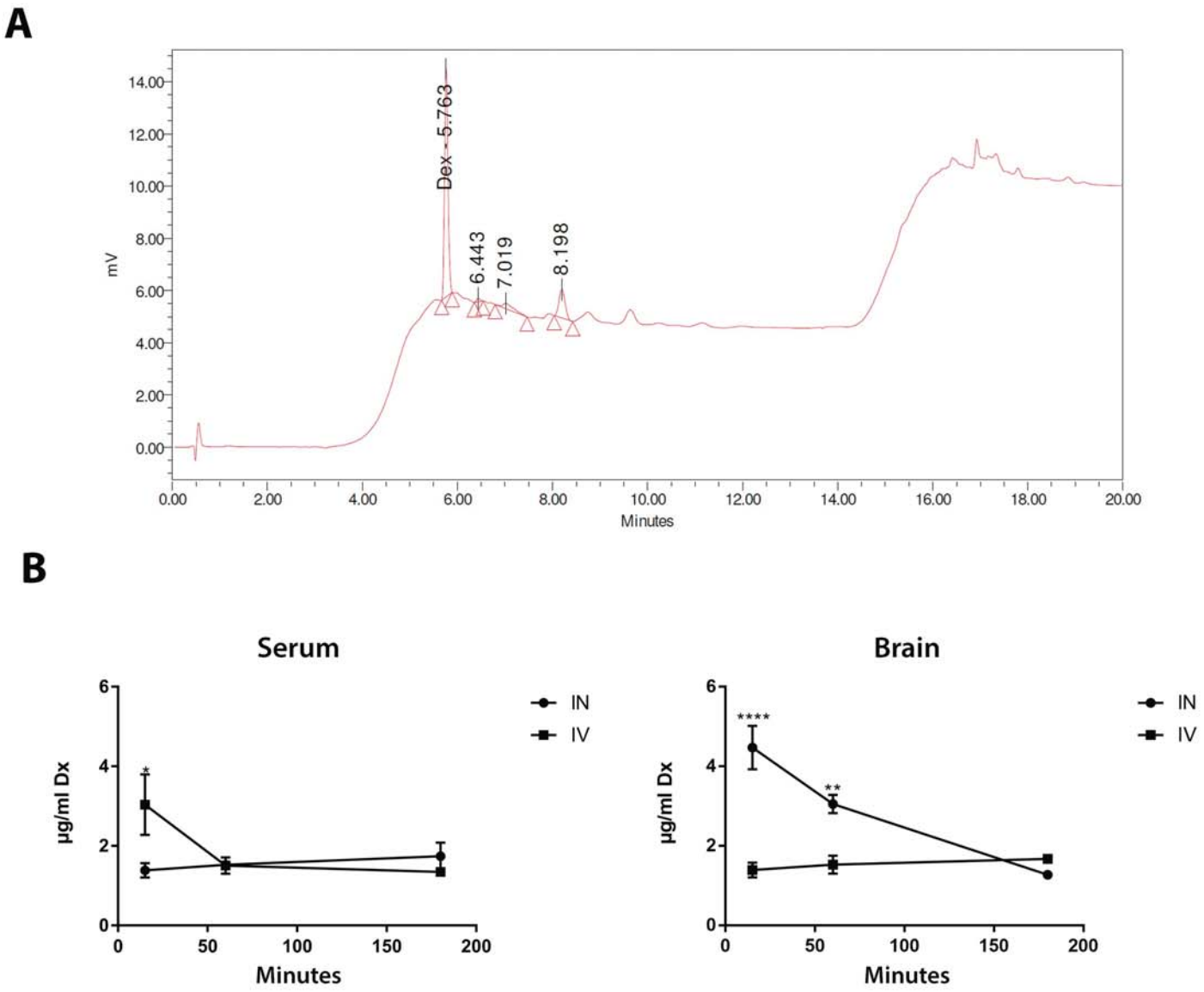

JPET Fast Forward. Published on June 16, 2021 as DOI: 10.1124/jpet.121.000530
This article has not been copyedited and formatted. The final version may differ from this version.